X-ray Structure of the Asn276Asp Variant of the *Escherichia coli* TEM-1 β-Lactamase: Direct Observation of Electrostatic Modulation in Resistance to Inactivation by Clavulanic Acid[†,‡]

Peter Swarén,[§] Dasantila Golemi,[||] Stéphanie Cabantous,[§] Alexey Bulychev,[||] Laurent Maveyraud,[§] Shahriar Mobashery,[||] and Jean-Pierre Samama*[,§]

Groupe de Cristallographie Biologique, Institut de Pharmacologie et de Biologie Structurale du CNRS, 205 route de Narbonne, 31077 Toulouse Cedex, France, and Department of Chemistry, Wayne State University, Detroit, Michigan 48202-3489

Received April 1, 1999; Revised Manuscript Received May 26, 1999

ABSTRACT: The clinical use of β-lactam antibiotics combined with β-lactamase inactivators, such as clavulanate, has resulted in selection of β-lactamases that are insensitive to inactivation by these molecules. Therefore, therapeutic combinations of an enzyme inactivator and a penicillin are harmless for bacteria harboring such an enzyme. The TEM β-lactamase variants are the most frequently encountered enzymes of this type, and presently, 20 variants are designated as inhibitor-resistant TEM ("IRT") enzymes. Three mutations appear to account for the phenotype of the majority of IRT enzymes, one of them being the Asn276Asp substitution. In this study, we have characterized the kinetic properties of the inhibition process of the wild-type TEM-1 β-lactamase and of its Asn276Asp variant with the three clinically used inactivators, clavulanic acid (clavulanate), sulbactam, and tazobactam, and we report the X-ray structure for the mutant variant at 2.3 Å resolution. The changes in kinetic parameters for the interactions of the inhibitors with the wild-type and the mutant enzymes were more pronounced for clavulanate, and relatively inconsequential for sulbactam and tazobactam. The structure of the Asn276Asp mutant enzyme revealed a significant movement of Asp276 and the formation of a salt bridge of its side chain with the guanidinium group of Arg244, the counterion of the inhibitor carboxylate. A water molecule critical for the inactivation chemistry by clavulanate, which is observed in the wild-type enzyme structure, is not present in the crystal structure of the mutant variant. Such structural changes favor the turnover process over the inactivation chemistry for clavulanate, with profound phenotypic consequences. The report herein represents the best studied example of inhibitor-resistant β-lactamases.

The β-lactam family of antibiotics includes many of the most extensively used antimicrobial agents in clinical medicine (*1*). Their importance stems from their antibacterial effectiveness, low toxicity, and predictable pharmacokinetics. Bacteria have developed several resistance mechanisms by which they counter the effects of antibiotics. The most common of these mechanisms is the β-lactamase-catalyzed hydrolytic opening of the β-lactam ring, which renders the antibiotic harmless to the bacteria. Two approaches have been used to counteract the action of β-lactamases. The first is to alter the structure of the β-lactam antibiotic in such a way that it becomes a poor substrate for these enzymes, but retains its ability to inactivate its biological targets, the penicillin-binding proteins (PBP).[1] The limitation of this strategy is the ever-increasing number of β-lactamase variants with extended substrate profiles (*2*, *3*). The plasmid-mediated TEM family provides the largest ensemble of these variants, and 67 such enzymes have been identified to date (http://www.lahey.org/studies/webt.htm) (*4*).

The discovery of clavulanic acid (*5*), a potent inactivator of the class A β-lactamases, allowed for a second viable strategy, where a β-lactam with high antibacterial activity would be coadministered with the β-lactamase inhibitor. However, 20 TEM variants, designated as inhibitor-resistant TEM ("IRT"), and one SHV variant have evolved showing less sensitivity to inactivation by one or more of the clinically used inhibitors, clavulanic acid (**1**), sulbactam (**2**), and tazobactam (**3**) (Figure 1).

The IRT enzymes were first described in 1992, simultaneously in France (*6*) and in the United Kingdom (*7*). The sites of amino acid substitutions leading to IRTs are different from those giving extended spectrum TEM mutant enzymes (*8*). Six positions seem to be prevalent: (i) Met69 can be substituted with leucine, isoleucine, or valine, (ii) Trp165 with arginine, (iii) Met182 with threonine, (iv) Arg244 with cysteine, serine, histidine, or leucine, (v) Arg275 with leucine or glutamine, and (vi) Asn276 with aspartic acid. However,

[†] The work in France was funded by the French Ministry of Education and Research, the Centre National de la Recherche Scientifique, and the Région Midi-Pyrénées (J.-P.S.). The work in the United States was supported by grants from the National Institutes of Health and the National Science Foundation (S.M.).

[‡] The crystallographic coordinates have been deposited in the Brookhaven Protein Data Bank under file name 1ck3.

* Corresponding author. E-mail: samama@ipbs.fr. Telephone: 33 5 61 17 54 44. Fax: 33 5 61 17 54 48.

[§] Institut de Pharmacologie et de Biologie Structurale du CNRS.

[||] Wayne State University.

[1] Abbreviations: rmsd, root-mean-square deviation; PBP, penicillin-binding proteins; IRT, inhibitor-resistant TEM.

10.1021/bi990758z CCC: $18.00
Published on Web 07/02/1999

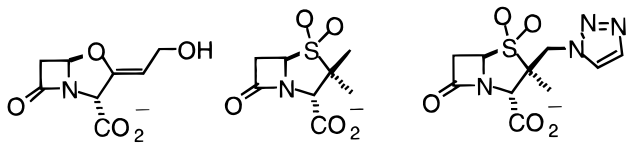

1 2 3

FIGURE 1: Chemical structures of the clinically used inhibitors of class A β-lactamases.

three of these sites are of major consequence for resistance to clavulanic acid (*9*). These sites are at positions 69 (*10*−*16*), 244 (*17*−*19*), and 276 (*12*, *14*, *20*).

Although the mutation Asn276Asp is always found coupled to another mutation at position 69 in natural IRT isolates (*12*−*14*), the engineered Asn276Asp mutation alone was shown to provide resistance to clinically used inhibitors (*9*, *20*, *21*). In this work, we report the detailed analysis of the kinetic parameters of inhibition of the Asn276Asp variant with the three clinically used β-lactamase inhibitors and the three-dimensional structure of the mutant enzyme. The combination of both kinetic and structural analyses allows the description of the subtle modifications of the enzyme leading to an inhibitor-resistant bacterial phenotype.

MATERIALS AND METHODS

The procedures for mutagenesis for the Asn276Asp mutant variant were reported previously (*9*). The wild-type TEM-1 β-lactamase and its Asn276Asp variant were purified by a known procedure (*22*). Penicillin G was purchased from Sigma, and clavulanate was obtained from the SmithKline Beecham Pharmaceutical Co. Sulbactam was obtained from Pfizer, and tazobactam was from Wyeth-Ayerst.

Kinetic Measurements. All kinetics measurements were performed on a Hewlett-Packard 8453 diode array spectrophotometer. Calculations of kinetic constants were performed by the MS Excel software. The assays were carried out by monitoring hydrolysis of penicillin G at 240 nm ($\Delta\epsilon_{240}$ = 570 M^{-1} cm^{-1}). The determination of the inhibition parameters was carried out at room temperature in 100 mM sodium phosphate buffer (pH 7.0). These experiments were performed under conditions of excess substrate concentrations, as described by Koerber and Fink (*23*). Inactivation constants for clavulanate and sulbactam were calculated for both the wild-type and mutant enzymes, according to Imtiaz et al. (*19*). Inactivation experiments were initiated by the addition of a portion of a stock solution of clavulanate or sulbactam (0.3−3 mM final concentration) to the enzyme (2 μM) solutions. The final concentration for tazobactam in inactivation experiments with the wild-type enzyme ranged from 8 to 42 μM and with the mutant enzyme from 60 to 300 μM. Incubation was stopped by dilution of 10 μL aliquots of an incubation mixture into a 1 mL assay containing 2 mM penicillin G, at various time intervals. The residual enzyme activity in the aliquot was monitored until the complete depletion of the substrate was observed. A progressive increase of the activity of the enzyme was observed initially, attributed to its recovery from the transiently inhibited species (*19*). The highest steady-states rates, during the course of substrate hydrolysis, were used in the calculation of the remaining enzyme activity.

The dissociation constants (K_I) for all three inhibitors were calculated for both the wild-type and Asn276Asp enzymes, by the method of Dixon (*24*). Two concentrations of the substrate penicillin G, typically 200 and 500 μM, were used, except in the case of tazobactam with the Asn276Asp mutant, where the penicillin G concentrations were 400 and 500 μM. A series of assay mixtures containing both substrate and various concentrations of the inactivators (2−24 μM for clavulanate, 2−30 μM for sulbactam, and 0.4−2 μM for tazobactam) were prepared in 100 mM sodium phosphate buffer (pH 7.0). An aliquot of the stock solution of the enzyme was added to afford a final concentration of 5 nM, for both the wild-type enzyme and the Asn276Asp mutant, in a total volume of 1.0 mL, followed by the immediate measurement of enzyme activity. The rates were measured for the first 5% of substrate turnover.

The value of k_{cat} for the Asn276Asp mutant enzyme for sulbactam was determined according to the procedure by Imtiaz et al. (*25*). The partition ratios (k_{cat}/k_{inact}) for clavulanate, sulbactam, and tazobactam were determined for both enzymes by the titration method (*26*). Several buffered mixtures containing various molar ratios of [I]/[E] of each of the inhibitors with each of the enzymes were incubated at 4 °C overnight (ca. 20 h). The molar ratio [I]/[E] for clavulanate was varied from 1 to 160 for the wild-type enzyme and from 1 to 120 for the Asn276Asp mutant. For sulbactam, the molar ratio was varied from 1 to 4000 for the Asn276Asp mutant, and the conditions for the experiments with the wild-type enzyme were reported previously (*25*). For tazobactam, the molar ratio was varied from 1 to 360 for the wild type and from 1 to 560 for the Asn276Asp mutant. The remaining activity of the enzyme was assayed under conditions of excess substrate, with penicillin G. The rate constants for recovery of enzyme activity (k_{rec}) from the transiently inhibited species for the wild-type and Asn276Asp enzymes incubated with each of the compounds were measured at the molar ratio ([I]/[E]) that gave the longest interval of time prior to arriving at a linear steady-state rate for hydrolysis of penicillin G. The calculations of the constants were performed according to the method of Glick et al. (*27*).

Crystal Preparation. Crystallization conditions were similar to those used for the wild-type TEM-1 (*28*). A drop of 2.5 μL mutant protein solution at 11.6 mg/mL in 70 mM sodium−potassium phosphate buffer (pH 7.8), containing 8.3% saturated ammonium sulfate, was equilibrated for 4 days against a reservoir containing 42% saturated ammonium sulfate and 4% acetone (v/v) in 100 mM sodium−potassium phosphate buffer at 4 °C. Thereafter, the equilibrated drop was seeded with a microcrystal of the wild-type TEM-1 washed in 47% saturated ammonium sulfate and 100 mM sodium−potassium phosphate (pH 7.8). Four days later, the ammonium sulfate concentration was increased to 43% saturation and, after an additional 4 days, to 44% saturation. Mutant crystals grow to a typical size of 200 μm × 400 μm × 600 μm. The procedure was repeated three times, using crystals of the mutant enzyme in the second and the third seeding experiments.

X-ray Data Collection and Processing. Diffracted intensities were collected at 4 °C from three crystals on an R-axis IIc system (λ = 1.5418 Å), and merged to give an 83% complete data set at 2.3 Å resolution with an *R*-merge of 3.8% (Table 1). The crystals belong to space group $P2_12_12_1$ with the following cell parameters: a = 41.8 Å, b = 60.4

Table 1: Data Processing and Refinement Statistics

	overall resolution range of 24.5−2.28 Å	highest-resolution shell of 2.34−2.28 Å
no. of observations	19,279	853
no. of independent reflections	8,771	416
multiplicity	2.2	2.1
completeness (%)	81.6	54.0
R_{merge}[a]	0.038	0.077
$\langle I/\sigma I\rangle$	25.2	15.1
R_{factor} of 0.165	R_{free} of 0.235	
1991 protein atoms ($\langle B\rangle = 22.2$ Å^2)	76 water molecules ($\langle B\rangle = 28.2$ Å^2)	
rms deviation		
bond lengths, 0.005 Å	bond angles, 1.2°	
dihedral angles, 22.3°	improper angles, 1.1°	

[a] $R_{merge} = \Sigma\Sigma|\langle I\rangle - I_i|/\Sigma\Sigma I_i$.

Å, and $c = 88.6$ Å. Diffraction data were processed using MOSFLM (*29*) and scaled and merged using ROTAVATA and AGROVATA from the CCP4 suite of programs (*30*).

Model Refinement. Rigid-body optimization using reflections between 8.0 and 3.0 Å (4044 reflections) and the wild-type structure (*31*) was performed using X-PLOR (*32*). Refinement, applying a bulk solvent correction, was carried out with no cutoff on diffraction data (24.5−2.3 Å, 8755 reflections) and electrostatic terms turned off. In the first refinement cycle, simulated annealing from 2000 to 300 K (0.5 fs time step) was followed by 80 steps of Powell energy minimization. In the next steps, manual corrections using the program O (*33*) were followed by simulated annealing refinement (from 600 to 0 K) and individual *B*-factor refinement. After inclusion of water molecules, the slow cooling scheme was abandoned for conventional refinement, including grouped occupancy refinement for the alternate conformation of the Met272 side chain. The final model contains 1999 protein non-hydrogen atoms and 76 water molecules. The *R* and R_{free} values were 0.158 and 0.234, respectively. The side chains of Lys55, Gln99, Lys111, Lys146, Glu197, Leu198, Lys215, and Lys256 had poorly defined electron densities.

RESULTS

Kinetics. Table 2 summarizes the kinetic measurements with the wild-type and mutant enzymes. An important difference between the two enzymes is that the Asn276Asp enzyme exhibits a 43-fold decrease in its affinity for clavulanic acid ($\Delta\Delta G$ of 2.2 kcal/mol). Furthermore, the inactivation rate constant (k_{inact}) for the mutant enzyme is reduced by 35%. As will be discussed, this is partly due to the absence of Wat402 in the active site of the Asn276Asp mutant enzyme (vide infra), which was suggested to be the source of an important proton in the inactivation chemistry of clavulanate (*19*). Therefore, the immediate product of enzyme acylation (**4**) would not readily lead to the linear acyl−enzyme species **7** (**4** → **5** → **6** → **7**), which results in enzyme inactivation (Scheme 1). As a consequence, species **4** is hydrolyzed more readily by the enzyme and turnover takes precedence over the inactivation chemistry.

The changes in the kinetic parameters for interactions of the two enzymes with sulbactam and tazobactam are relatively less significant. One of the exceptions is the K_I value for tazobactam with the two enzymes. The affinity for tazobactam of the wild-type enzyme, as measured by K_I, is high (20 nM), but like the case of clavulanate, the mutant enzyme exhibits a 20-fold lower affinity ($\Delta\Delta G = 1.8$ kcal/mol). However, since the affinity for the wild-type enzyme is so high to begin with, the concentration of the inhibitor near the K_I value for the mutant enzyme is still attainable in vivo. Resistance to this inhibitor, if seen, should be relatively weak, in line with the IC_{50} measurements (*21*). The second exception is the k_{inact} for sulbactam, which has been enhanced 10-fold for the mutant enzyme. The k_{inact} value for sulbactam with the mutant enzyme becomes similar to that of clavulanate with the wild-type enzyme. However, since k_{cat} is also enhanced by 4-fold, the partition ratio (k_{cat}/k_{inact}) is still high (4000) for the mutant enzyme.

Structural Analysis. The overall structure of the mutant protein is almost identical to the structure of the wild-type enzyme (*31*). The backbone atoms from both structures can be superimposed with an rmsd of 0.26 Å, which is not distinguishable from the expected coordinate errors at this resolution. However, a global superimposition may obscure subtle structural differences, and the two protein structures were compared using the matrix resulting from the superimposition of all atoms of the catalytically critical residues, Ser70, Lys73, Ser130, Glu166, and Lys234, and of those defining the oxyanion hole, the main chain nitrogen atoms of Ser70 and Ala237 (the rmsd for these atoms was 0.25 Å). We found that the mutation induced a concerted displacement along the β-sheet surface of C-terminal α-helix H11 (residues 272−290), of N-terminal α-helix H1 (residues 26−40), and of 3_{10}-helix H10 (residues 219−224) (Figure 2). The rmsd over all backbone atoms of these residues was 0.52 Å, when compared to the wild-type structure.

Aspartate 276, which belongs to helix H11, is displaced by 0.75 Å (rmsd over all atoms) with respect to the position of Asn276 in the wild-type protein. On the contrary, the position of the guanidinium moiety of Arg244, which interacts with the side chain of residue 276, has virtually not been modified (Figure 2). In the mutant protein, Arg244 and Asp276 form a tighter interaction than do Arg244 and Asn276 in the wild-type enzyme. In the TEM-1 β-lactamase (Figure 3a), the Asn276 Oδ1 atom interacts with both atoms Nϵ (2.9 Å) and Nη2 (3.2 Å) of the guanidinium group of Arg244. This atom and the carbonyl oxygen atom of Val216 bind the water molecule (Wat402) that was proposed to be the source of proton in the inactivation process by clavulanate (Scheme 1). The Arg244 Nη1 atom is hydrogen bonded (3.1 Å) to one of the oxygen atoms of the sulfate anion provided by the crystallization medium.

The distance between Asp276 Oδ1 and Arg244 Nϵ atoms is shorter (2.7 Å) in the Asn276Asp mutant enzyme (Figure 3b), but the main cause of the tighter interaction arises from a new interaction between Asp276 Oδ2, and Arg244 Nη2 atoms (3.3 Å). These atoms were at a distance of 4.3 Å in the wild-type enzyme. Hence, while residues 244 and 276 were only linked by hydrogen bonding in the wild-type enzyme, they are linked by both salt bridge and hydrogen bond interactions in the Asn276Asp mutant enzyme.

In contrast to the wild-type TEM-1 β-lactamase, there is no sulfate ion bound in the active site of the Asn276Asp enzyme, although ammonium sulfate was present at an identical concentration for protein crystallization. A water

Table 2: Kinetics Parameters for the TEM-1 Wild Type and Asn276Asp Mutant

enzyme	inhibitor	k_{cat} (s^{-1})	k_{inact} (s^{-1})	K_I (μM)	k_{cat}/k_{inact}	k_{rec} (s^{-1})
wild-type	clavulanate	$(0.21 \pm 0.03) \times 10^{-1}$	$(1.7 \pm 0.3) \times 10^{-3}$ [a]	0.4[b]	125 ± 36	$(8.4 \pm 0.1) \times 10^{-3}$
	sulbactam	1.95 ± 0.15[c]	2.0×10^{-4} [c]	1.6[c]	1×10^{4} [c]	$(1.12 \pm 0.02) \times 10^{-2}$
	tazobactam	1.4 ± 0.9	$(3 \pm 2) \times 10^{-3}$	$(2 \pm 1) \times 10^{-2}$	475 ± 42	$(7.23 \pm 0.05) \times 10^{-3}$
N276D mutant	clavulanate	0.16 ± 0.03	$(1.1 \pm 0.2) \times 10^{-3}$ [a]	17 ± 1.6	141 ± 7	$(3.2 \pm 0.6) \times 10^{-2}$
	sulbactam	8 ± 1	$(2 \pm 1) \times 10^{-3}$ [d]	6.1 ± 0.3	4000[e]	$(3.3 \pm 0.2) \times 10^{-2}$
	tazobactam	2.1 ± 0.5	$(2.2 \pm 0.5) \times 10^{-3}$	0.4 ± 0.1	933 ± 87	$(1.32 \pm 0.02) \times 10^{-2}$

[a] The discrepancies in the k_{inact} values from those reported by Saves et al. (*20*) are due to the transiently inhibited species observed during the inactivation of both enzymes by clavulanate, and also due to the methods used for calculating the k_{inact}; Saves et al. calculated k_{inact} from the half-times of inactivation at saturating concentrations of the inactivator, whereas in this study, k_{inact} values were obtained from double-reciprocal plots of the determinations of k_{obs} at various concentrations of clavulanate. These differences in procedures contribute to the discrepancies in the values of partition ratios as well. [b] Imtiaz et al. (*19*). [c] Imtiaz et al. (*25*). [d] The k_{inact} values were calculated from k_{cat} and k_{cat}/k_{inact}. [e] Imtiaz et al. (*19*) (footnote a) observed product inhibition during the determination of this parameter, which manifested itself in a deviation from linear kinetics. Therefore, they defined the partition ratio as the ratio of inhibitor to enzyme in which a 90% loss of activity was seen, and this is how the partition ratio is defined for sulbactam in this report.

Scheme 1

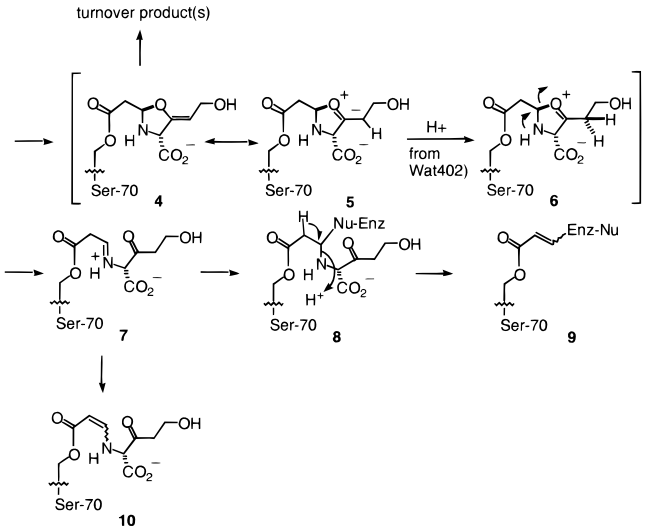

molecule is found in this area, at hydrogen bond distance to the Arg244 Nη1 atom (3.5 Å). Finally, although a weak electron density appeared in the vicinity of the carbonyl oxygen of Val216 during the refinement process, a water molecule corresponding to Wat402 in the wild-type structure could not be crystallographically refined in the Asn276Asp structure. This observation indicates a low or transient occupancy of this water molecule at this site.

DISCUSSION

On initial modification of the active site of β-lactamase, clavulanate partitions in three separate ways (Scheme 1). It may be turned over, as would any substrate for β-lactamase; it may function as a transient inhibitor, and it may also result in irreversible inactivation of the enzyme. Hydrolysis of the compound takes place presumably at the initial acyl−enzyme species (**4**). However, if the five-membered ring of this species opens up (**4** → **5** → **6** → **7**), species **7** may proceed to either transient inhibition (**10**) or irreversible inactivation (**9**). This species may be processed further (*34*). These processes take place with comparable rates in the case of the TEM-1 β-lactamase and have been discussed in more detail elsewhere (*19*, *35*). It should be noted that both pathways (to transient inhibition and irreversible inactivation) require the initial protonation of the oxonium moiety (**5**). This critical proton is likely delivered by the water molecule (Wat402) located, in the X-ray structure of the wild-type enzyme (*31*), between the Nη2 atom of the guanidinium group of Arg244 and the carbonyl oxygen atom of Val216 (Figure 3a).

Despite relatively modest kinetic effects, the substitution of asparagine by aspartic acid has profound phenotypic attributions on enzyme inhibition (for analysis of minimum-inhibitory concentrations of β-lactam antibiotics in the presence of clavulanate for all the known IRTs, see ref *9*). They arise from a significant local alteration of the electrostatic properties of the protein. In the TEM enzyme, residue 276 is located on C-terminal α-helix H11. Its mutation generates new interactions with Arg244, and unexpectedly, the seemingly facile displacement of the Arg244 side chain is not seen (Figure 2). These interactions involve a significant change in the position of residue 276, which likely drives the displacement of the entire H11 helix, and thus of helices H1 and H10, located on each side of H11 (Figure 2). The displacement of these three helices, which are involved in crystal packing interactions, may explain the rather large shift in cell parameters for the crystals of the mutant protein (a = 41.8 Å, b = 60.4 Å, and c = 88.6 Å) compared to those for the wild-type crystals (a = 43.1 Å, b = 64.4 Å, and c = 91.2 Å). This coordinated movement of almost 40 residues could not have been predicted from molecular modeling, which suggested the formation of a salt bridge interaction between Arg244 and Asp276, but assumed a movement of the Arg244 side chain (*20*, *21*).

The enhanced interactions between Arg244 and Asp276 in the mutant enzyme lead to a significant decrease in the positive electrostatic potential generated by Arg244. It is illustrated by two features in the structure of the Asn276Asp mutant enzyme and has important mechanistic implications. Despite the identical crystallization conditions, there was no evidence for the binding of a sulfate ion in the active site of the mutant enzyme, in contrast to its occurrence in the wild-type enzyme (*31*, *36*) (Figure 3). By studying the derivatives of the electrostatic potential generated by the wild-type enzyme, Swáren et al. (*37*) showed that the position of this anion in the crystal structure corresponds to a local maximum of the positive electrostatic potential. Accordingly, in the known X-ray structures of acyl−enzyme complexes of the TEM enzyme (*38*−*41*), the carboxylate group of substrates or of mechanism-based inhibitors was found in this position. These observations are consistent with the earlier comments of Moews et al. (*42*) and measurements by Zafaralla et al.

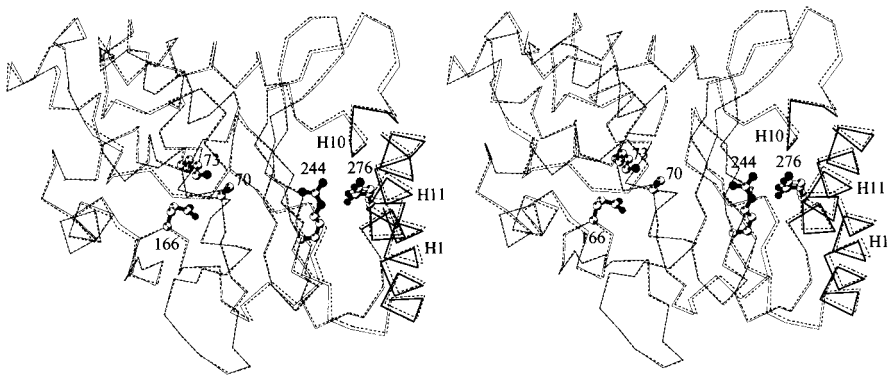

FIGURE 2: Stereoview of the Cα traces of the wild-type TEM-1 enzyme (···) and of the Asn276Asp mutant protein. Helices H1, H10, and H11 are shown for the mutant enzyme with thick lines. The residue at position 276 in both structures is represented as a ball and stick (black for the Asn276Asp mutant enzyme). Catalytic residues (Ser70, Lys73, and Glu166) and Arg244 are also denoted. This figure was generated with Molscript (*46*).

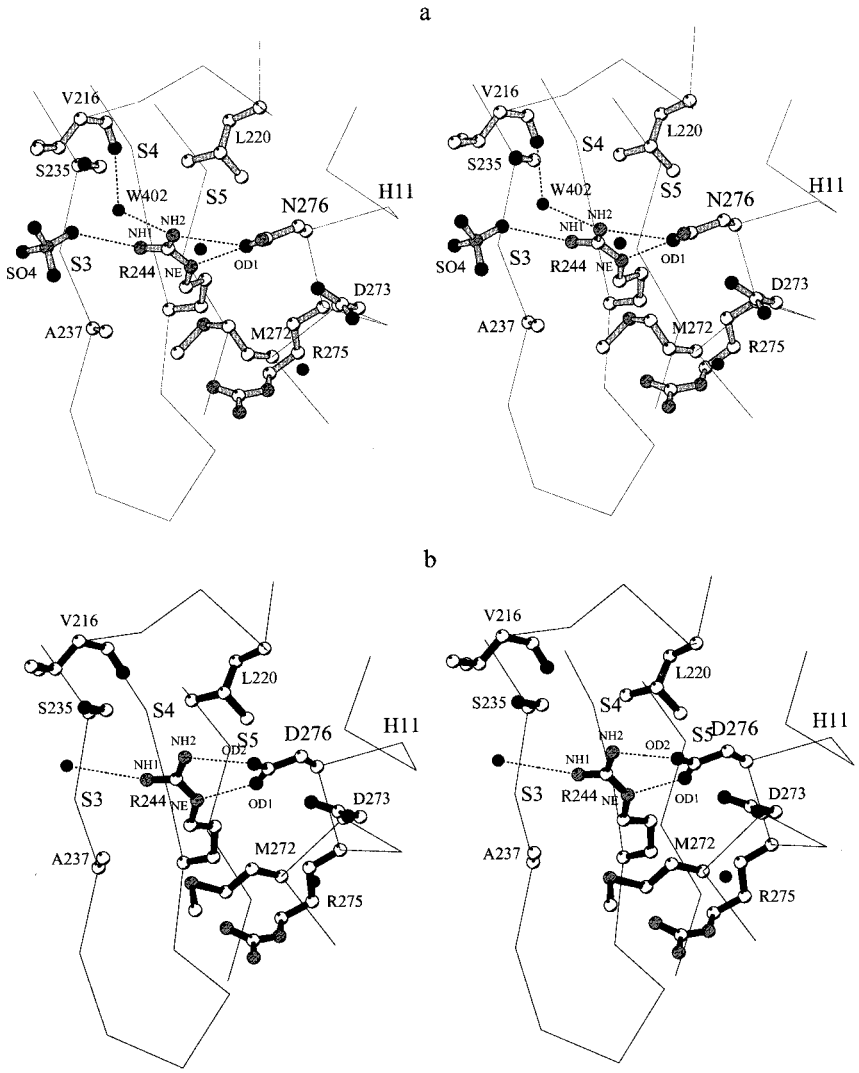

FIGURE 3: Close view of the region around position 276. The Cα traces of the secondary structure elements are labeled, and water molecules are represented by black dots. (a) A network of polar contacts in the structure of the wild-type enzyme. The sulfate anion is also represented. (b) Polar interactions in the structure of the Asn276Asp mutant enzyme. This figure was generated with Molscript (*46*).

(*22*), who had proposed that Arg244 may serve as the counterion for the carboxylates of the substrates and inactivators on binding of these compounds to the active site. The significant "neutralization" of the guanidinium group of Arg244 by the carboxylate group of Asp276 could thus explain the decreased affinity for all substrates (*20*) and inhibitors (a contribution evaluated to be approximately 2 kcal/mol; Table 2).

Another feature pertinent to the decrease in the positive electrostatic potential, and related to the kinetic and phenotypic effects of the Asn276Asp mutation, is the much reduced occupancy of the water molecule at hydrogen bond distance

to Arg244 and Val216, despite the spatial conservation of its ligand atoms in the mutant enzyme. This water molecule, clearly defined in the wild-type structure, appears to be only transiently present in the mutant structure. Imtiaz et al. (*19*) pointed out that this crystallographic water molecule located in the same position in the *Bacillus licheniformis* 749/C (*43*) and *Escherichia coli* TEM-1 (*31*) β-lactamases may be the source for protonation of species **4**. This offered a plausible explanation for the activity of the IRTs with substitutions at position 244, such as the clavulanate-resistant R244C/S/H TEM mutants. Deletion of the guanidinium group would affect the position of the water and/or the occupancy of the site by the water molecule, and therefore impair protonation of **4**. It is hence interesting to observe in the structure of the Asn276Asp TEM mutant enzyme the fact that the presence of a water molecule in this location appears to be transient, consistent with the measured attenuation of 35% in k_{inact} for the mutant enzyme with clavulanate. The immediate product of enzyme acylation (**4**) would be more rapidly hydrolyzed and would thus not readily lead to the inactivating species **7** (**4** → **5** → **6** → **7**). It is important to restate that since Wat402 in the wild-type enzyme would make a hydrogen bond to the carboxylate of clavulanate in both the preacylation complex and the acyl−enzyme intermediate (*19*), its absence should also be expected to contribute to the lowered affinity of the mutant enzyme for inhibitors, such as seen in this case (Table 2).

The Asn276Gly mutant of the OHIO-1 β-lactamase, an SHV-type class A enzyme, was designed and studied recently (*44*). Bonomo et al. also reported a decrease in the affinity of the mutant enzyme for clavulanate, although the effect of the mutation on the rate constant for enzyme inactivation was not studied. As reported in this paper, the effect of mutation in the TEM β-lactamase appears to be both a reduction in affinity for clavulanate and an attenuation of the rate constant for enzyme inactivation. In light of the fact that the Asn276Gly mutant of the OHIO-1 β-lactamase would not be able to have the specific interactions between Arg244 and Asp276 shown in our crystal structure, its contribution to the drug resistance phenotype is most likely due to the lack of the ability of Gly276 to sequester the side chain of Arg244, and by consequence the critical water molecule for the inactivation chemistry, such as proposed by Bonomo et al. previously (*44*).

CONCLUSIONS

Earlier modeling suggested that the Asn276Asp substitution would decrease the electrostatic potential in the area where the carboxylate group of a substrate binds, and hence should contribute to the lower affinity observed with the mutant enzyme. The lack of sulfate in the mutant crystal structure confirms that there is indeed a decrease in the electrostatic potential. However, the structural changes by which the mutant enzyme decreases the occupancy of Wat402 without changing the hydrogen-bonding pattern were entirely unforeseen.

One appreciates that a single amino acid change may in principle have dramatic effect on the protein structure. One such example is the long-known classic example of the mutant hemoglobin from sickle-cell anemia (*45*). Such a dramatic effect is not operative in the example at hand in this paper. This report serves as a hallmark in subtleties of protein structure and enzyme function. The first inspection would indicate that the mutation does not appear to have made a significant structural modification of the enzyme, and that it does not have the ability to have direct (first solvation shell) interaction with the ligand bound in the active site. The influences of residue 276 are indeed subtle and indirect. But the effects are sufficient to influence the phenotypic manifestation of resistance to inactivation by clavulanate (*9*). Indeed, a notable increase in the minimum inhibitory concentration (MIC) for organisms harboring the Asn276Asp mutant has been reported (*21*).

It is important to note that the kinetic measurements of the mutant enzyme do not point to a profound alteration of the properties of the enzyme. However, it would appear that the modulation of the properties of the enzyme is just sufficient for the purpose. This is a relatively minor structure modification, which gives resistance to inactivation by the clinical inactivator, yet retains the enzyme as a resistance factor so it can serve its normal function in turnover of typical β-lactam substrates.

We hasten to add that it is a comfort that the manifestation of the reduced propensity to inactivation observed with the Asn276Asp mutant is seen only for clavulanate. In principle, the resistant organisms that harbor this mutant enzyme can be treated with clinical preparations of the antibiotics with the other two inactivators. This may indeed be approaching the limit of what nature would be able to accomplish without tampering entirely with the catalytic function of the resistance enzyme. However, this statement should be tempered by acknowledging that selection of mutants in bacterial populations in clinical setting is extremely powerful, and we may indeed run into novel mutations, which would potentially affect all three clinical inhibitors in the future.

ACKNOWLEDGMENT

We thank Lionel Mourey for his interest in this work and for stimulating discussions.

REFERENCES

1. Bush, K., and Mobashery, S. (1998) in *Resolving the antibiotic paradox. Progress in understanding drug resistance and development of new antibiotics* (Rosen, B. P., and Mobashery, S., Eds.) pp 71−98, Plenum Press, New York.
2. Philippon, A., Labia, R., and Jacoby, G. A. (1989) *Antimicrob. Agents Chemother. 33*, 1131−1136.
3. Jacoby, G. A., and Medeiros, A. A. (1991) *Antimicrob. Agents Chemother. 35*, 1697−1704.
4. Franceschini, N., Perilli, M., Segatore, B., Setacci, D., Amicosante, G., Mazzariol, A., and Cornaglia, G. (1998) *Antimicrob. Agents Chemother. 42*, 1459−1462.
5. Brown, A. G., Butterworth, D., Cole, M., Hanscomb, G., Hood, J. D., Reading, C., and Rolinson, G. N. (1976) *J. Antibiot. 29*, 668−669.
6. Vedel, G., Belaaouaj, A., Gilly, L., Labia, R., Philippon, A., Névot, P., and Paul, G. (1992) *J. Antimicrob. Chemother. 30*, 449−462.
7. Thomson, C. J., and Amyes, S. G. B. (1992) *FEMS Microbiol. Lett. 91*, 113−118.
8. Knox, J. R. (1995) *Antimicrob. Agents Chemother. 39*, 2593−2601.
9. Vakulenko, S. B., Geryk, B., Kotra, L. P., Mobashery, S., and Lerner, S. A. (1998) *Antimicrob. Agents Chemother. 42*, 1542−1548.

10. Delaire, M., Labia, R., Samama, J.-P., and Masson, J.-M. (1992) *J. Biol. Chem. 267*, 20600−20606.
11. Blazquez, J., Baquero, M.-R., Canton, R., Alos, I., and Baquero, F. (1993) *Antimicrob. Agents Chemother. 37*, 2059−2063.
12. Brun, T., Péduzzi, J., Caniça, M. M., Paul, G., Névot, P., Barthélémy, M., and Labia, R. (1994) *FEMS Microbiol. Lett. 120*, 111−118.
13. Zhou, X. Y., Bordon, F., Sirot, D., Kitzis, M.-D., and Gutmann, L. (1994) *Antimicrob. Agents Chemother. 38*, 1085−1089.
14. Henquell, C., Chanal, C., Sirot, D., Labia, R., and Sirot, J. (1995) *Antimicrob. Agents Chemother. 39*, 427−430.
15. Stapleton, P., Wu, P.-J., King, A., Shannon, K., French, G., and Phillips, I. (1995) *Antimicrob. Agents Chemother. 39*, 2478−2483.
16. Farzaneh, S., Chaibi, E. B., Péduzzi, J., Barthélémy, M., Labia, R., Blazquez, J., and Baquero, F. (1996) *Antimicrob. Agents Chemother. 40*, 2434−2436.
17. Bret, L., Chaibi, E. B., Chanal-Claris, C., Sirot, D., Labia, R., and Sirot, J. (1997) *Antimicrob. Agents Chemother. 41*, 2547−2549.
18. Belaaouaj, A., Lapoumeroulie, C., Caniça, M. M., Vedel, G., Névot, P., Krishnamoorthy, R., and Paul, G. (1994) *FEMS Microbiol. Lett. 120*, 75−80.
19. Imtiaz, U., Billings, E. M., Knox, J. R., Manavathu, E. K., Lerner, S. A., and Mobashery, S. (1993) *J. Am. Chem. Soc. 115*, 4435−4442.
20. Saves, I., Burlet-Schiltz, O., Swarén, P., Lefèvre, F., Masson, J.-M., Promé, J.-C., and Samama, J.-P. (1995) *J. Biol. Chem. 270*, 18240−18245.
21. Caniça, M. M., Caroff, N., Barthélémy, M., Labia, R., Krishnamoorthy, R., Paul, G., and Dupret, J.-M. (1998) *Antimicrob. Agents Chemother. 42*, 1323−1328.
22. Zafaralla, G., Manavathu, E. K., Lerner, S. A., and Mobashery, S. (1992) *Biochemistry 31*, 3847−3852.
23. Koerber, S. C., and Fink, A. L. (1987) *Anal. Biochem. 165*, 75−87.
24. Dixon, M. (1953) *Biochem. J. 55*, 170−171.
25. Imtiaz, U., Billings, E. M., Knox, J. R., and Mobashery, S. (1994) *Biochemistry 33*, 5728−5738.
26. Silverman, R. (1988) *Mechanism-based enzyme inactivation: chemistry and enzymology*, CRC Press, Boca Raton, FL.
27. Glick, B. R., Brubacher, L. J., and Leggett, D. J. (1978) *Can. J. Biochem. 56*, 1055−1057.
28. Jelsch, C., Lenfant, F., Masson, J.-M., and Samama, J.-P. (1992) *J. Mol. Biol. 223*, 377−380.
29. Leslie, A. G. W. (1987) Profile fitting, in *Computational aspects of protein crystal analysis. Proceedings of the Daresbury Study Weekend* (Helliwell, J. R., Machin, P. A., and Papiz, M. Z., Eds.) pp 39−50, Daresbury Laboratory, Warrington, U.K.
30. Collaborative Computational Project Number 4 (1994) *Acta Crystallogr. D 50*, 760−763.
31. Jelsch, C., Mourey, L., Masson, J.-M., and Samama, J.-P. (1993) *Proteins 16*, 364−383.
32. Brünger, A. T. (1992) *X-PLOR version 3.1. A system for X-ray crystallography and NMR*, Yale University Press, New Haven, CT.
33. Jones, T. A., Zou, J. Y., Cowan, S. W., and Kjeldgaard, M. (1991) *Acta Crystallogr. A 47*, 110−119.
34. Fisher, J., Charnas, R. L., and Knowles, J. R. (1978) *Biochemistry 17*, 2180−2184.
35. Massova, I., and Mobashery, S. (1997) *Acc. Chem. Res. 30*, 162−168.
36. Fonzé, E., Charlier, P., To'th, Y., Vermeire, M., Raquet, X., Dubus, A., and Frère, J.-M. (1995) *Acta Crystallogr. D 51*, 682−694.
37. Swarén, P., Maveyraud, L., Guillet, V., Masson, J.-M., Mourey, L., and Samama, J.-P. (1995) *Structure 3*, 603−613.
38. Strynadka, N. C. J., Adachi, H., Jensen, S. E., Johns, K., Sielecki, A., Betzel, C., Sutoh, K., and James, M. N. G. (1992) *Nature 359*, 700−705.
39. Maveyraud, L., Massova, I., Birck, C., Miyashita, K., Samama, J.-P., and Mobashery, S. (1996) *J. Am. Chem. Soc. 118*, 7435−7440.
40. Strynadka, N. C. J., Martin, R., Jensen, S. E., Gold, M., and Jones, J. B. (1996) *Nat. Struct. Biol. 3*, 688−695.
41. Maveyraud, L., Mourey, L., Kotra, L. P., Pédelacq, J.-D., Guillet, V., Mobashery, S., and Samama, J.-P. (1998) *J. Am. Chem. Soc. 120*, 9748−9752.
42. Moews, P. C., Knox, J. R., Dideberg, O., Charlier, P., and Frère, J.-M. (1990) *Proteins 7*, 156−171.
43. Knox, J. R., and Moews, P. C. (1991) *J. Mol. Biol. 220*, 435−455.
44. Bonomo, R. A., Dawes, C. G., Knox, J. R., and Shlaes, D. M. (1995) *Biochim. Biophys. Acta 1247*, 121−125.
45. Harrington, D. J., Adachi, K., and Royer, W. E. J. (1998) *J. Mol. Biol. 272*, 398−407.
46. Kraulis, P. J. (1991) *J. Appl. Crystallogr. 24*, 946−950.

BI990758Z